Skin model of pollutants penetration
helps demonstrate the protective activity of a natural water

Cenizo Valérie[1*]; Lemaire Géraldine[1] ; Olivero Malvina[1] ; Rouquet Virginie[1] ; Decombe Clément[2] ; Robin Sophie[2] ; Portes Pascal[1].

[1] L'Occitane en Provence - L'Occitane Group, Manosque, France ; [2] Biotoskin, Besançon, France ; [3] Bioexigence, Besançon, France

* Cenizo Valérie, Laboratoires M&L ZI Saint-Maurice 04100 Manosque, 0033492702600, valerie.cenizo@loccitane.com

Abstract

Background: The exposition of skin to air pollutants has been associated with skin cancer, inflammation and allergy. The skin permeability barrier prevents penetration of chemicals from the environment, but large amounts of airborne pollutants can overwhelm it and even alter it. We demonstrated that Réotier water (RW) reinforces the permeability barrier. To test whether RW was able to prevent pollutants penetration, we setup a pollutants penetration assay using a living skin model in culture.

Methods: Skin explants placed in a Franz cell-like device with a receptor compartment containing culture medium, were sprayed daily with RW and Trans-Epidermal Electrical Resistance (TEER) was measured for 7 days. Other skin explants pre-treated or not with RW, were exposed to pollutants. Pollutants penetration, skin viability, TEER and gene expression analysis were monitored.

Results: in control skin, RW increased TEER from 5 hours to day 7. Pollution disrupted the barrier as shown by decreased TEER values. RW protected the skin barrier, reduced the penetration of pollutants and prevented cytotoxicity. Pollution activated the Aryl hydrocarbon receptor pathway and xenobiotic metabolization signaling and increased the expression of genes related to cell death, apoptosis and necrosis. RW pretreatment stimulated the expression of genes related to cell viability and survival pathways and decreased those related to cell death, apoptosis and necrosis.

Conclusion: This model of pollutants penetration on a living skin in culture allowed to demonstrate that Réotier water can enhance the skin permeability barrier in just a few hours and limit pollutants penetration and their toxicity on skin.

Keywords: Pollution; skin barrier; water; skin model; tight junction

Introduction

The increase of air pollution, associated with rapid economic growth and industrialization, has a major impact on human health. Environmental air pollutants are generated by the industrial activity, the combustion of fuel, but can also come from indoor pollutants like paints, glues and cigarette smoke. Natural sources of pollution include volcanic ash, wildfires. They are composed of a heterogeneous mixture of suspended gases, liquids and solids and are classified according to their physicochemical properties [1]: particulate matter (PM), and gazes. Gazes are represented for example by ozone (O_3), carbon monoxide (CO) and volatile organic compounds (VOCs). PM is classified by diameter, coarse (PM_{10} 2,5-10 µm), fine ($PM_{2.5}$ <2,5 µm) and ultrafine (< 0,1 µm) and composed of a mixture of organic compounds such as polycyclic aromatic hydrocarbons (PAHs) and inorganic compounds such as heavy metals bound to it.

Numerous studies have shown that long-term effects of ozone and particulate matter exposure are associated with cardiovascular and respiratory mortality and morbidity [2,3]. The skin, like the lung tissue, is at the interface between the body and the atmosphere and therefore is in direct contact with pollutants. The exposition of skin to air pollutants has been associated with serious effects such as skin cancer, as well as inflammatory and allergic skin conditions [4]. Vierkötter et al. were the first to demonstrate in 2010 that chronic exposure to PM led to premature skin aging, particularly pigment spot formation [5].

Moreover, PAH can easily penetrate the skin and further alter the skin barrier function [6]. They are the main ligand of the Aryl hydrocarbon receptor (AhR), a potent transcription factor expressed by both keratinocytes and melanocyte. AhR activation was shown to induce the production of pro-inflammatory mediators, increase the production of reactive oxygen

species (ROS) [7] and induce transcriptional expression of genes which are of known relevance for pigment spot and wrinkle formation [8-10].

The skin permeability barrier prevents penetration of chemicals from the environment. It is ensured firstly by the lipids in the *stratum corneum (SC)* and secondly by the intercellular junctions between keratinocytes. In particular, tight junctions are believed to be the second barrier after the *stratum corneum.*

Calcium plays a pivotal role in the formation of this barrier function. There is a calcium gradient within the epidermis, from a low level of calcium ions in the basal and spinous layers, followed by a progressive increase with a level of calcium ions reaching its maximal density within the *stratum granulosum* [11,12]. Already in 1980 it was shown that a concentration of 1.44 mM calcium chloride is sufficient to drive keratinocytes into differentiation [13]. An increase in the calcium level is also necessary for proper functioning of adherent junctions, allowing the binding of E-cadherin on one cell to E-cadherin on a neighboring cell [14, 15], and tight junctions, inducing the deposition of their protein components to the cell membrane [16].

But large amounts of airborne pollutants can overwhelm the skin's protective abilities and even alter the barrier function, accelerating pollutants penetration. It is therefore necessary to develop protective shields for the skin and active ingredients that help strengthen skin's natural defense.

Réotier water (RW) is a calcium-rich natural water from the French Alps, which has been used since ancient times to cure and soothe skin conditions. We previously showed on human reconstructed epidermis that RW could reinforce the permeability barrier by inducing tight junctions and cornified envelope proteins expression and limited the penetration of the Lucifer yellow [17].

The goal of this study was to test whether RW, by reinforcing the skin barrier formation, could limit the penetration of pollutants into the skin and therefore limit their deleterious effect.

Materials and Methods.

D-skin cell® device

The D-Skin cell® model is a hermetic cell in PMMA and Teflon. This device is composed of a lower part (6 wells with water bath) and an upper part (hermetic cover). Each skin sample was deposited in horizontal position on insert of culture, creating two compartments, one on each side of the sample: a donor compartment ("epidermal" compartment) consisting of a PMMA cylinder with an open surface of 3.14 cm², applied to the upper side of the skin, a receptor compartment containing 7 ml of receptor fluid.

Skin explants and donors

For the skin barrier evaluation study, abdominal skin explants from 3 donors (42, 55 and 55 years old) were placed in the device, 3 explants per donor and condition. Skin explants were maintained in culture (37°C, 5% CO2) for 7 days.

For the pollutants penetration study, abdominal skin explants from 3 donors (31, 43 and 49 years old) were placed in the device, 3 explants per donor and condition. Skin explants were maintained in culture for 2 days.

RW and pollutants application

For the skin barrier evaluation study, in the absence of pollution, RW was sprayed daily (3 sprays) on the surface of half of the explants and the other half was untreated. When the skin surface was dry (15 min), the explants were placed in the incubator (37°C, 5% CO_2).

For the pollutants penetration study, skin explants were treated as described in *figure 1.* The pollution mix was composed of 50 µg benzo(a)pyrene (B(a)P, 25 µg dibenzoanthracene (DBA), 10 µl benzene, 12,5 µl $PM_{2.5}$ and 12,5 µl PM_{10}. Titanium (Ti) and Lead (Pb) were selected as major components of $PM_{2.5}$ and PM_{10} and represented 15 ppm and 12 ppm of the pollution mix respectively.
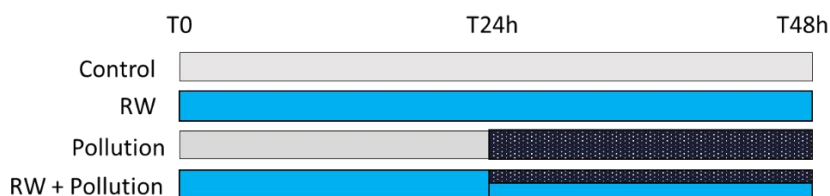
Figure 1: Protocol of prevention of pollutants penetration experiment using the D-Skin Cell device.
Skin explants were placed in the device (right panel). Control condition received no treatment. RW
condition was sprayed with RW (3 sprays) à T0 and T24h. Pollution condition was exposed to the
pollution mix at T24h. RW+Pollution was pre-treated with RW at T0 and at T24h just before exposure
to the pollution mix. Culture medium was replaced by PBS with PEG 6%. Skin explants were
maintained in culture for an additional 24 hours.

Pollutants penetration analysis

Skin samples collection

4h, 6h, 8h, 10h, 12 and 24h after exposure to pollution, 500 µl of receptor medium were
sampled for pollution assay. Samples were kept at -20°C until assay. 500 µl of PBS with
PEG were then put back in wells. The dilution factor was taken into account in the
calculations.

24 hours after exposure to pollution, a cotton bud was used over the surface of each skin
samples in order to obtain the pollution remaining (washing). Cotton bud was cut and then
put into 20 ml glass tube. A D-Squame was then applied over the surface of each disc under
a constant controlled pressure (80 g/cm²). D-Squame (*stratum corneum*) was placed in an
Eppendorf. Dermo-epidermis separation was carried out using forceps. Epidermis were
weighted and put in an Eppendorf. Dermis were weighted and put into 20 ml glass tube.
Tubes were stored at -20°C until treatment and analysis.

HPLC assay for benzo(a)pyrene and dibenzanthracene

Extraction of pollutants was carried out for the surface, *stratum corneum* (SC), epidermis,
and dermis assay. 1.5 ml of extraction solvent (acetone/water, 50/50) were placed is each vial
prior to 24h stirring. Samples were filtered prior to injection. The HPLC system was an

Agilent Technologies-Chromatographic Equipment: 1260 Infinity II. The column was a C18 (25 cm × 4.6 mm) with pore size of 5 µm (Supelcosil^{TM} LC-PAH). The mobile phase was water/acetonitrile (gradient 0/100-0,01min, 35/65-15 min, 15/85- min, 5/95-5 min, 0/100-15 min) with a flow rate of 1.2 ml/min. The column was maintained at 30°C. The injection volume was 20 µl and the wavelength was 254 nm. The method was linear for a coefficient of correlation r²>0.999. Receptor fluid samples were injected with no specific preparation and dilution.

GC-MS assay for benzene

Approximately 1g of sample was placed in a glass test tube. HCl and 2,2-imethoxypropane were added to the tube and heated for 30 min at 100°C. Sample was centrifuged and injected to the GC-MS system. The column was a 20 m x 0.18 mm ID InertCap 17 narrow bore column with 0.18-µm film thickness. Helium was used as the carrier gas at flow rate of 1 ml/min. The temperatures of the injection port and transfert line were set at 250°C and 300°C respectively. The oven temperature was set at 100°C for 0.5 min and then increased to 300°C to the rate of 20°C/min. The LOD was 4 µg and LOQ was 5 µg.

ICP-MS for Titanium and Lead

Approximately 1g of sample was transferred to a Teflon digestion vessel and 5 ml nitric acid + 1 ml of purified water was added to each vessel. The vessels were placed in a microwave oven for the digestion. After digestion, the resulting solution was fixed with 20 ml of purified water. The Ti and Pb concentrations in the samples were measured by ICP-MS. The amount of Ti and Pb was calculated using a standard curve of Ti or Pb. ICP-MS conditions for Ti and Pb were listed below:

Condition	Titanium (Ti)	Lead (Pb)
Radiofrequency power (W)	1600	1075
Mode	Single	Dual
Nebulization flow (ml/min)	0.95	0.90
Auxiliary gas flow (L/min)	1.2	1.2
Plasma gas flow (L/min)	16	15

The LOD and LOQ were respectively for Ti 0.06 ppm and 0.1 ppm and for Pb 0.02 ppm and 0.04 ppm.

Skin viability

24h after exposure to pollutants, a punch of 3 mm of diameter was done on each skin explant. Viability study was performed using a MTT test. Each sample was placed in an Eppendorf containing 450 µl of medium and 50 µl of MTT. The tubes were then incubated at 37°C for 4 hours. Formazan blue created by the process was then extracted with 500µl of DMSO. After an overnight incubation at 37°C, optical density was read with multiscan spectrophotometer at 550 nm. Cell viability was expressed in percentage in comparison of the cell viability of the control. A condition was considered cytotoxic when viability was below 80% of the control.

Trans-epithelial electrical resistance (TEER) measurement

Each sample was put on gauze. Trans epidermal electrical resistance was then measured. Each skin sample was placed on an electrode covered with cotton embedded PBS. 100 µl of PBS were also put over the surface of the skin. The second electrode was then put into contact with PBS. Then a current of 100Hz was applied between the two probes. The more the skin was damaged, the less was the resistance. TEER measurement was expressed in kΩ.

DNA microarray

Skin explants were collected 24 hours after exposure to pollution, placed in 3 ml of RNA later and then frozen at -80°C (9 samples per condition (3 replicates-3 donors).

RNA extraction

For each sample, a small piece of skin (90–100 mg) was disrupted and homogenized using Omni Tissue Homogenizer into TRIzol® reagent. The upper phase was transferred to RNeasy spin columns and total RNA was extracted using mini-RNeasy kits (Qiagen, Courtabœuf, France) according to the manufacturer's instructions, with the addition of the DNase digestion step. RNA quality/integrity and concentration were assessed using an Agilent 2100 Bioanalyzer (Agilent Technologies, Les Ulis, France) and NanoDropTM Spectrophotometer (Thermo Fisher Scientific, Asnières-sur-Seine, France), respectively.

Preparation and hybridization of probes

The total RNA (100 ng) of each sample was reverse transcribed, amplified and labeled with Cyanine 3 (Cy3) as instructed by the manufacturer of the One-Color Agilent Low Input Quick Amp Labeling Kit (Agilent Technologies, Les Ulis, France). Cy3-labeled cRNA was hybridized onto Agilent Whole Human Genome Oligo 8X60K V2 Arrays (SurePrint G3 Human Gene Expression 8x60K v2 Microarray Kit, G4851B; 50,599 probes) using reagents supplied in the Agilent Hybridization kit (One-Color Microarray-based Gene Expression Analysis Protocol). The slides were scanned with the Agilent SureScan Microarray Scanner System. The one-color microarray images were extracted with Feature Extraction software (v12.0.0.7), which performs background subtractions and generates a quality control report.

Microarray analysis

Raw data produced from microarrays were imported into GeneSpring GX13.0 software (Agilent) to determine the differentially expressed genes between treated and control samples. The raw data were normalized and filtered by flag using GeneSpring GX13.0 software. The normalization included log2 transformation, per chip normalization to 75% quantile and dropped per gene normalization to median. Flag filtering included genes that were at least detected in 100 percent of the samples in either condition. In addition, GeneSpring GX13.0 software was used to filter a set of pollution- or pollution+RW-responsive genes for which the expression levels were significantly modified (unpaired moderated t-test, $p<0.05$), with an average fold change ≥ 1.5 or ≤ -1.5 compared to the control group and pollution plus RW-responsive genes were filter against pollution one with the same filter. Those results were adjusted for multiple testing by the false discovery rate (FDR) with the Benjamini–Hochberg procedure using a threshold of 0.05. RW responsive-genes for which the expression level were significantly modified (unpaired t-test, $p<0.05$) with an average fold change ≥ 1.5 or ≤ -1.5 were compared to the control group, without adjusted for multiple testing by the FDR. Outcomes from microarray analysis in Genespring GX13.0 software were uploaded into Ingenuity Pathway Analysis (IPA, Qiagen, Redwood City, CA) system for core analysis and then overlaid with the global molecular network in the Ingenuity Pathway Knowledge Base (IPKB). To determine the top biological functions associated with the observed gene expression profiles, we performed a downstream and upstream effect

analysis from which we extracted the affected functions (p-value ≤ 0.05). The right-tailed Fisher's exact test was used to estimate the probability that association between a set of molecules and a function or pathway might be due to random chance. The IPA regulation z-score algorithm was used to predict the direction of change for a given function (increase or decrease). A positive z-score means that a function is significantly increased whereas a negative z-score indicates a significantly decreased function.

Claudin-1 immunohistochemistry

Skin explants were collected 24 hours after exposure to pollution. A punch of 5 mm of diameter was placed in an Eppendorf tube containing formol (10%) for histology. After 30 min fixation in formol and rinsing in PBS, biopsies were dehydrated and embedded in paraffin. 6-µm paraffin sections were dewaxed and rehydrated. Sections were incubated with anti-claudin 1 rabbit polyclonal antibody (Abcam, Ab15098) overnight at 4°C in humid atmosphere. After extinction of endogenous peroxidases (10% H_2O_2, 15 min), secondary antibody (Histofine F/414151F, MM France) coupled to Horse Radish Peroxidase was incubated for 30 min at room temperature. DAB chromogene allowed to reveal the labelling. Counterstaining was performed with Mayer's haematoxylin. As a negative control, primary antibody was removed. Slides were dehydrated in Ottix plus (F/X0073, MM France) and mounted in Diamount mounting medium (F/030400, MM France). 3 representative pictures of each sample were taken with Zeiss LSM880 microscope.

Statistical analysis

Data management and statistical analyses were accomplished using GraphPad Software (La Jolla, California, USA). To assess statistical differences between experimental groups, a RM two-way the analysis of variance (ANOVA) was performed for TEER kinetic assay in the absence of pollution. For pollution penetration studies (chemicals quantification, TEER and viability), paired Student t-test was performed between control and treated conditions.

Results

RW rapidly reinforces the skin barrier function

Our previous results on the properties of RW showed that it could increase the expression of epidermal differentiation proteins (i.e involucrin, filaggrin and claudin-1) in reconstructed human epidermis and decrease the penetration of small molecules like Lucifer yellow [17]. We thus hypothesized that RW could improve the skin barrier function through the stimulation epidermal differentiation. To test this hypothesis, we sprayed RW on the surface of skin explants placed in a Franz cell-like device, the D-Skin cell, allowing the maintenance of the explants in culture. As expected, when sprayed daily on the skin surface, RW increased TEER values after 3 and 7 days in culture (+47% vs control, *figure 2*). More surprisingly, this increase could be observed as soon as 5 hours after the first treatment (+31%).
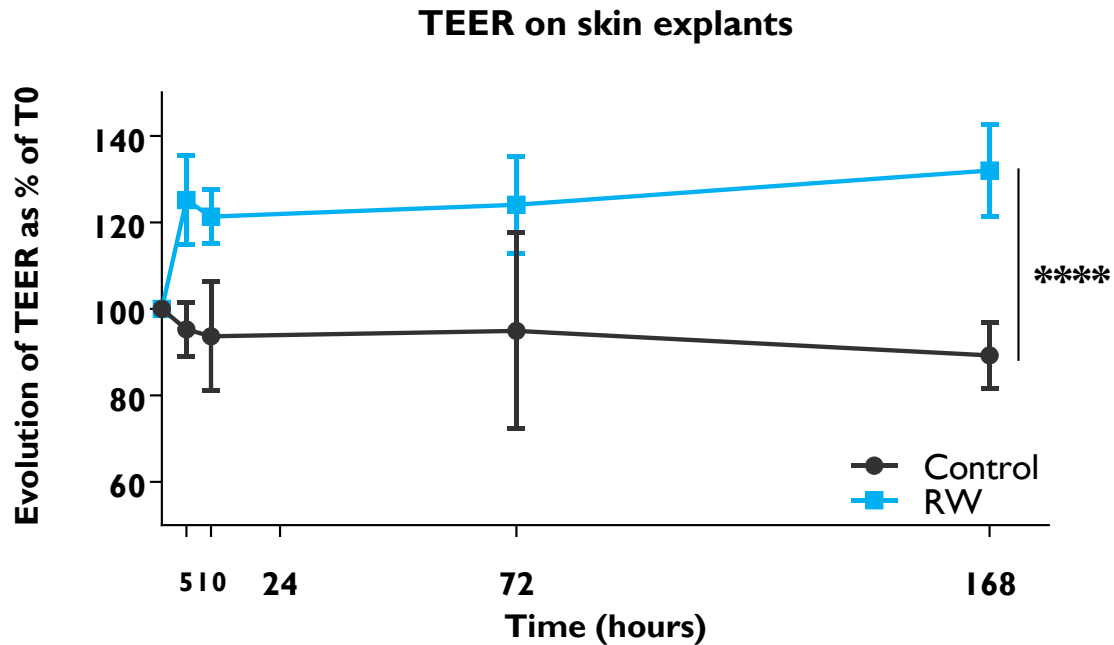

*Figure 2: Evaluation of the skin barrier with trans-epidermal electrical resistance (TEER). RW-treated explants in blue, control in black. Plotted values represent the mean of 3 explants per donor and 3 donors. ****p<0,0001 RM Two-way ANOVA (time and treatment) analysis.*

RW limits pollutants penetration

TEER reflecting the functionality of the tight junctions [16], the second skin barrier after *stratum corneum*, the increase observed suggested that RW could prevent small molecules penetration more rapidly than previously envisaged. We therefore tested the potential of RW to prevent pollutants penetration into the skin, only 24 hours after RW-treatment.

In this study, RW was sprayed on the skin surface 24 hours before, and again just before application of a mixture of various pollutants. This mixture reflected the diversity of atmospheric pollutants: polycyclic aromatic hydrocarbons (PAH) with benzo(a)pyrene and dibenzanthracene, volatile organic compounds (VOC) with benzene and $PM_{2.5}$ and PM_{10} containing heavy metals adsorbed on it, such as Ti and Pb [18,19]. The penetration these different molecules was followed in kinetics in the receptor medium, and after 24 hours in the different compartments of the skin.

Regarding the two PAH, Benzo(a)pyrene and dibenzanthracene, none of these molecules reached the receptor medium as they were not detected at any time point analyzed. Both were more detected in the non-absorbed part (washing) and in the epidermis. Benzo(a)pyrene was found in significantly lower quantity in the SC and epidermis of the RW-treated explants while dibenzanthracene was significantly less detected in the epidermis of RW-treated explants (*Figures 3 and 4*).

Benzene, due to its volatility, was analyzed by GC-MS. This molecule could not be detected neither in the receptor medium nor in the dermal compartment, suggesting it was stopped at the epidermal level. Its higher concentration in the skin was found in the SC. In RW-treated explants, benzene was found in significantly higher concentrations in the washing (no penetration) while in significantly lower amounts in the SC and epidermal compartments, confirming a decreased skin penetration (*Figure 5*).
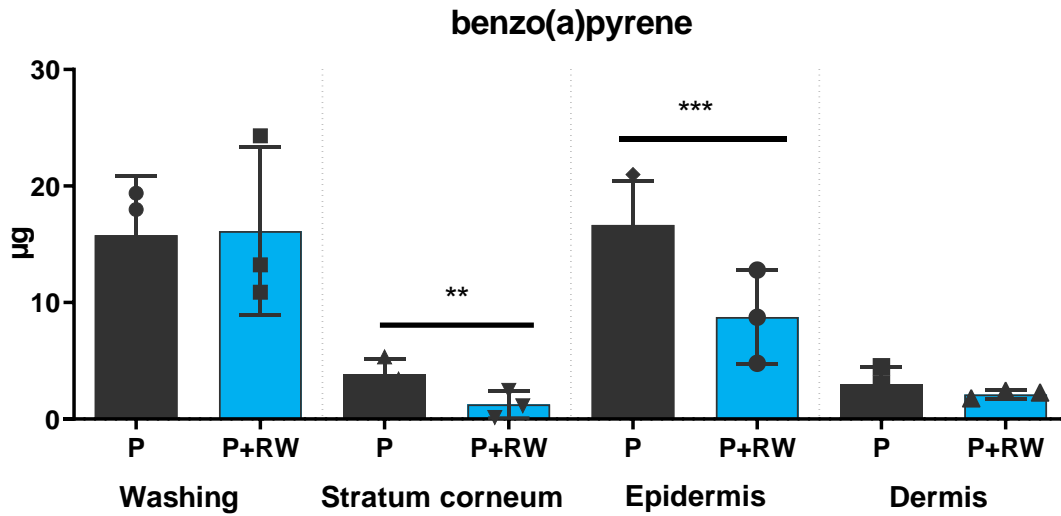
Figure 3: Penetration of benzo(a)pyrene in the skin compartments*. RW-pretreated explants in blue (P+RW), Pollution control in black (P). Plotted values represent the mean of 3 explants per donor and 3 donors. **p<0.01; ***p<0.001 paired Student t-test.*
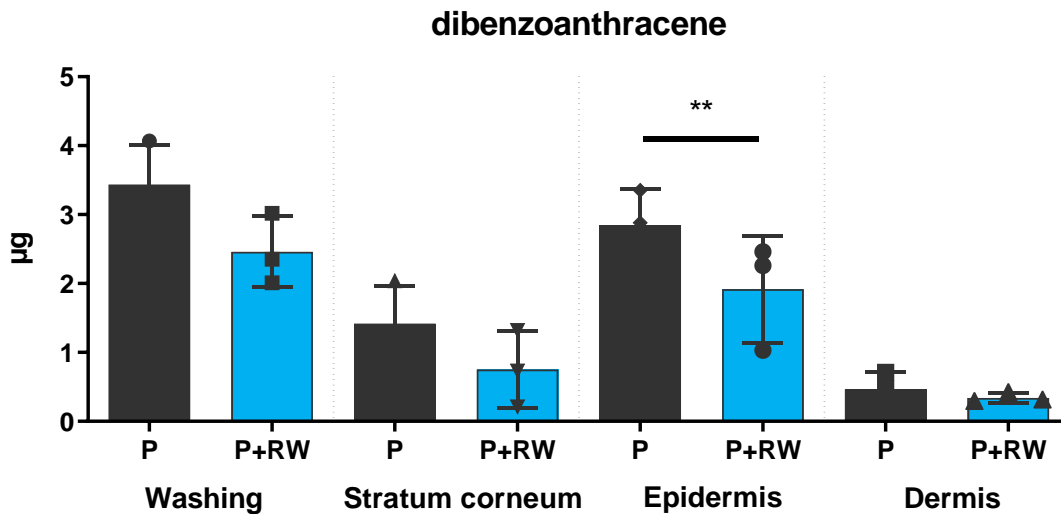

Figure 4: Penetration of dibenzanthracene in the skin compartments*. RW-pretreated explants in blue (P+RW), Pollution control in black (P). Plotted values represent the mean of 3 explants per donor and 3 donors. **p<0,01 Paired Student t-test.*
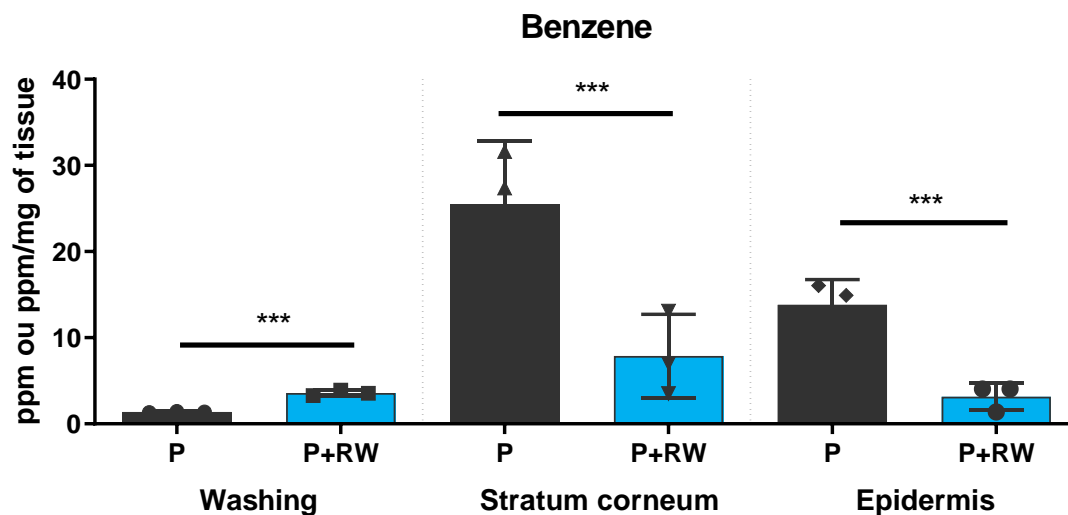
Benzene

Figure 5: Penetration of benzene in the skin compartments. RW-pretreated explants in blue (P+RW), Pollution control in black (P). Plotted values represent the mean of 3 explants per donor and 3 donors. ***p<0,001 Paired Student t-test

Finally, lead (Pb) and titanium (Ti) which are smaller molecules than PAHs and VOCs, could deeply penetrate through the skin and reach the receptor medium. In this compartment, lead was not detectable before 24 hours (***Figure 6***) while titanium was detected as soon as 8 hours after exposure and showed increasing concentration over time (***Figure 7***). In the RW-treated explants, the penetration of these two heavy metals was slowed down. In addition, their concentration was significantly decreased in all the skin compartments while increased in the washing.
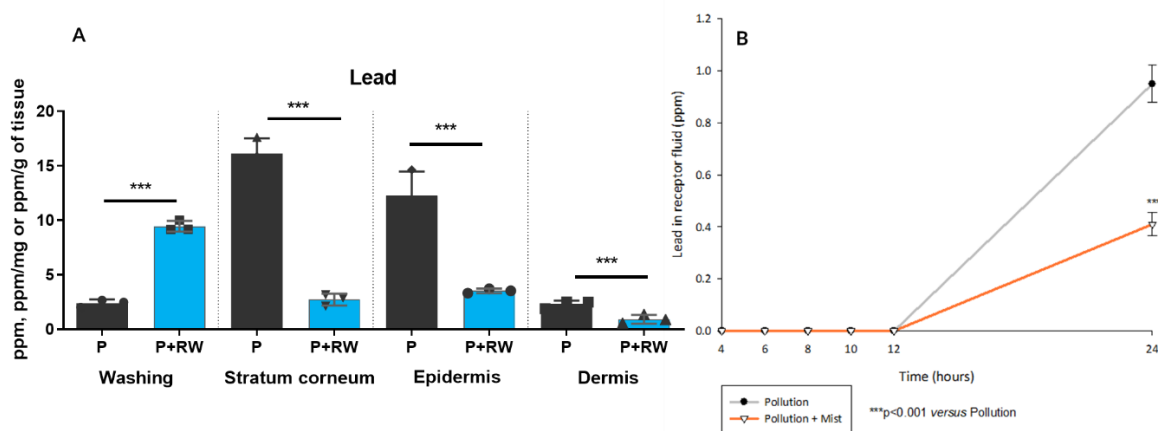
*Figure 6: Penetration of Lead (Pb) on PM$_{2.5}$ an PM$_{10}$. **A**- Penetration in the skin compartments after 24h. RW-pretreated explants in blue (P+RW), Pollution control in black (P). **B**- Penetration kinetics in the receptor medium. Plotted values represent the mean of 3 explants per donor and 3 donors. ***p<0.001 Paired Student t-test.*
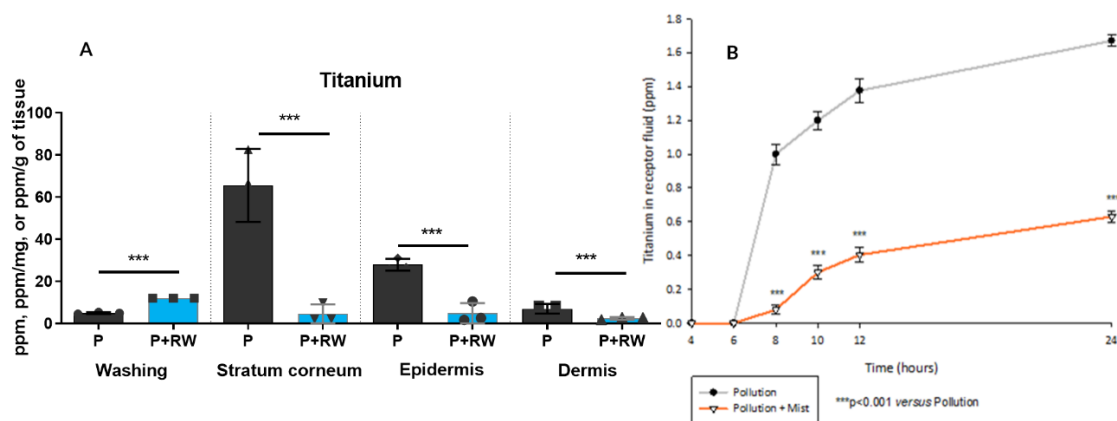

*Figure 7: Penetration of Titanium (Ti) on PM$_{2.5}$ an PM$_{10}$. **A**- Penetration in the skin compartments after 24h. RW-pretreated explants in blue (P+RW), Pollution control in black (P). **B**- Penetration kinetics in the receptor medium. Plotted values represent the mean of 3 explants per donor and 3 donors. ***p<0.001 Paired Student t-test.*

RW prevents pollution-induced barrier disruption

To verify our hypothesis of a rapid reinforcement of the tight junction barrier upon RW treatment, we tested the TEER on the skin samples (***Figure 8***). Compared to the control skin

in which TEER values remained stable during the 2 days kinetic, the RW treatment indeed increased TEER after 24 h. When pollution was added on the skin surface, it provoked a 15% decrease in the TEER values, suggesting a barrier disruption. When explants were pre-treated with RW before pollution exposure, the barrier integrity was maintained, as TEER values were not decreased under the values of the control skin.

Interestingly, 24 hours exposure to pollutant was not sufficient to induce a visible loss of tissue integrity (*Figure 8*, right panel) or a change in the tissular localization of claudin-1, one of the main components of tight junctions. At this timepoint, RW did not increase the level of claudin-1 expression, suggesting that the barrier improvement observed could not be explained by a protein synthesis increase.
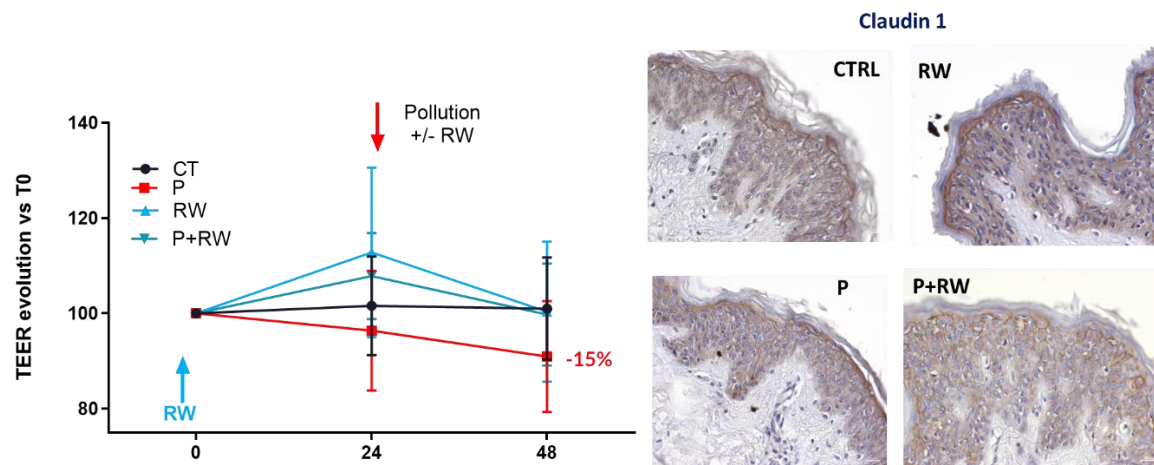

Figure 8: Effect of pollutants on skin barrier and tissue integrity. A- TEER values reflecting tight junctions barrier. Plotted values are normalized to the values of the control skin at Day 0 (100%). B- Claudin 1 immunostaining, claudin-1 in brown, hematoxylin tissue counter-staining in purple, magnification x200. CT: control skin, P: pollution-exposed, RW: RW-treated, P+RW: RW pre-treated and pollution exposed.

RW protects skin from pollution-induced cytotoxicity

To further analyze the skin's response to pollutants and the protective effect of RW preventive treatment, we performed a viability assay (*Figure 9*). Pollution significantly reduced skin cells viability (-20%) while RW-treated explants viability stayed similar to the control. RW-treatment also prevented pollution-induced cell cytotoxicity.
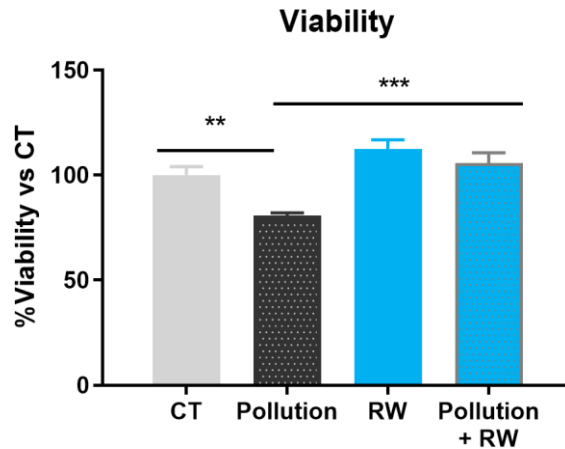
Figure 9: Effect of pollutants and RW-pretreatment on skin viability. *MTT assay. Plotted values are normalized to the values of the control skin at Day 0 (100%). **p<0.01; ***p<0.001 Paired Student t-test.*

To understand further how skin reacted to pollution and how RW prevented cell cytotoxicity, we then performed a transcriptomic analysis using Agilent Whole Human Genome Oligo Microarrays 8x60K V2 on skin explants exposed to pollution with or without RW-treatment. The significantly modulated genes (unpaired Student t-test, adjusted for multiple testing by the FDR <0,05) were scrutinized with IPA (Qiagen, Redwood City, CA, USA), which highlighted several diseases and functions with positive (increased) or negative (inhibited) activation z-scores. **Figure 10** depicts these modulated pathways. Numerous functions related to cell death, apoptosis, necrosis, tissue hypoplasia and DNA damage were upregulated by the exposure to pollution. On the contrary, functions involved in cell viability, cellular organization, transcription and cell cycle (mitosis, M phase) were downregulated confirming a strong pollution-induced cytotoxicity. When compared to the samples exposed to pollution alone, the explants pre-treated with RW and exposed to pollution presented significant inhibition of gene pathways related to functions such as necrosis, apoptosis while functions linked to transcription, cell viability and cell cycle (mitosis) were increased. These data confirmed that the RW-treatment prevented, at least in part the pollution-induced cytotoxicity. This protection was not complete as pathways related to cellular organization, such as cytoplasm organization, cytoskeleton organization or microtubule dynamics were all inhibited compared to pollution.
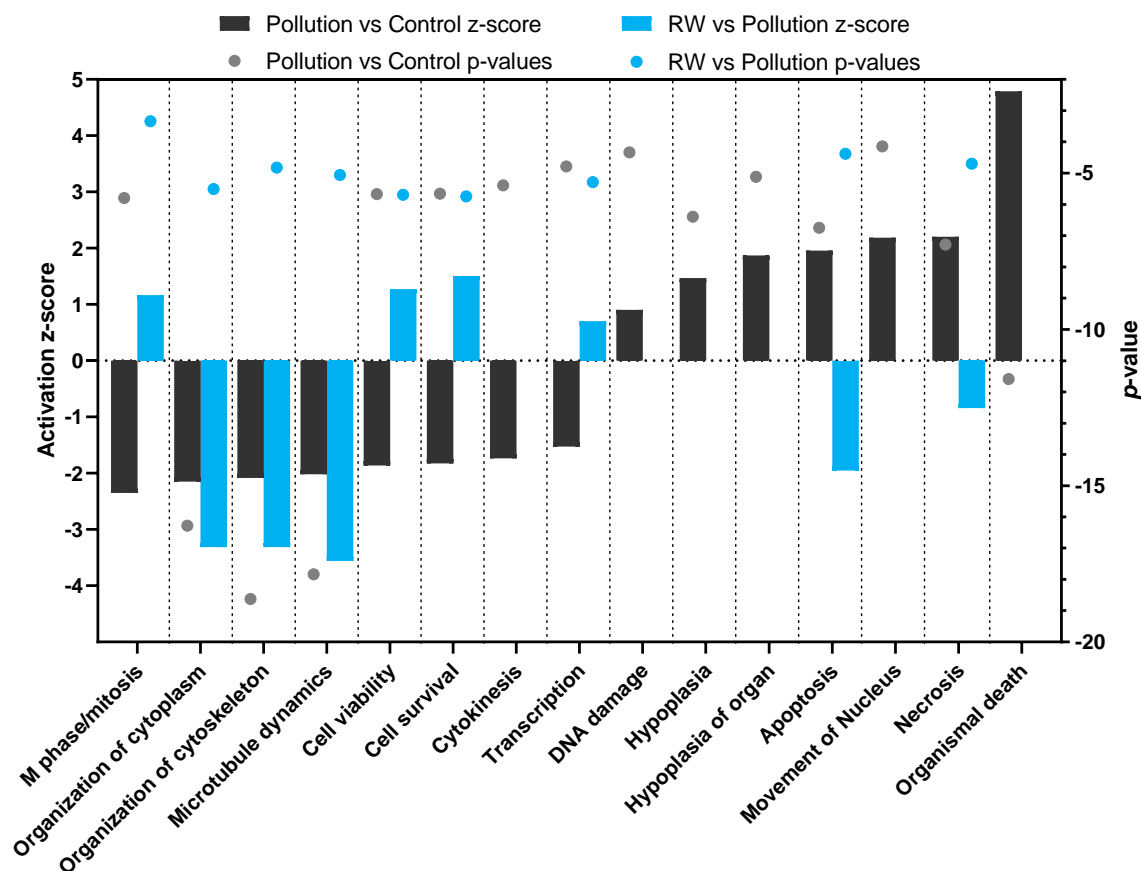
Figure 10: Transcriptomic analysis. *The activation z-score from Ingenuity Pathway Analysis algorithm (Qiagen) allows the identification of significant modulated biological functions. Z-scores are plotted as histogram bars. A positive z-score reflects an induction of the biological function while a negative z-score reflects an inhibition. The absence of bar for RW vs pollution reflects the absence of significant modulation of the listed functions in RW+P-treated explants compared to the pollution-exposed explants. The p-value (dots), calculated with the Fisher's exact test reflects the likelihood that the association between a set of genes in our dataset and a biological function is significant (p-value<0,05)*

Discussion

The analysis of molecules penetration on one hand, and skin response to pollutants on the other hand, require different time points, and for that reason they are usually performed separately, the penetration of pollutants being assessed with analytical methods on explants maintained at room temperature on a non-nutritive solvent, and the analysis of skin's

response on skin models in culture. Both methods have disadvantages. First, the penetration studies must be performed immediately after skin explants recovery from surgery, to limit the tissue degradation. They therefore cannot be pre-treated with active ingredients. Besides, the analysis of skin's response to pollutants is mostly performed on skin cells in 2D culture or on 3D reconstructed epidermis or full-thickness skin [20,21]. While these models are useful for deciphering the mechanisms by which a specific pollutant induces toxicity, they do not fully reflect how normal skin will react to pollutants. The barrier function of the 3D models in particular, is less robust than that of the normal human skin and could let penetrate more pollutants than normal skin. In this study, we developed a model of pollutants penetration in a living normal human skin. Being able to maintain the skin explants in culture for up to 7 days allowed us to study, not only chemicals penetration like in a classical Franz cell, but also to follow the impact of pollutants and an active ingredient on the same skin after several days.

We previously demonstrated that thanks to its high calcium concentration, RW could induce keratinocytes differentiation and barrier formation in a reconstructed epidermis [17]. Here, we found that its barrier-enhancing action appeared too early to be explained by the increased expression of skin barrier proteins, as shown by the absence of induction of claudin-1 protein while skin barrier was improved. Jouret F et al. showed that calcium participates in the tight junction (TJ) assembly via the calcium-sensing receptor (CaSR). Upon activation by high calcium concentrations, the CaSR triggers TJ protein ZO-1 to sites of cell-cell contact localization to the cell membrane in less than 1 hour [16]. We hypothesize that RW could act in a two-stages way to reinforce the skin barrier: an instant action via the reinforcement of the TJ structure with the proteins already present in the keratinocytes, and a long-term action via the stimulation of the differentiation process that will lead to a stronger *stratum corneum*. Although the hydro-lipidic film and the *stratum corneum* ensure most of the skin barrier function, some pollutants such as PAH have lipophilic properties and easily diffuse through the skin surface lipids [22]. Tight junctions serve as both outside-in and inside-out barriers, and impede paracellular movements of ions, water, macromolecules and microorganisms [23]. This second barrier is thus required to prevent lipophilic molecules penetration, as SC alone fails to do so.

The transcriptomic analysis of regulated pathway clearly showed the toxic effect of pollutants. Given the composition of the pollution mixture used in our study, its is highly conceivable that, together with oxidative stress, AhR activation was the main activated pathway. Indeed, benzo(a)pyrene and dibenzanthracene are two PAH and known AhR ligands. Benzo(a)pyrene interaction with AhR was shown to induce inflammation and DNA damage in keratinocytes [24]. The DNA damage function was increased in the pollution-exposed skin, as well as the apoptosis and necrosis functions. These two mechanisms are activated to eliminate damaged cells and prevent cancer formation. Both Benzo(a)pyrene and dibenzanhtracene are classified as a carcinogens and could trigger these genes regulations. Interestingly, a unique action on the skin barrier with RW-pre-treatment was able to reduce barrier disruption, decrease pollutants penetration and their consequences on skin toxicity. These observations offer new perspectives for the development of protective cosmetic formulas. They should offer a "shield-like" physical protection to prevent the initial contact of pollutants with the skin surface. Antioxidants should also be added to scavenge the ROS generated by the pollutants that have actually penetrated the living layers of the skin. Finally, solutions that increase the tight junction barrier should also be considered as they offer a complementary action between the preventive action of the surface shield and the curative action of antioxidants in the skin.

Conclusion

This model of pollutants penetration on a living skin in culture allowed to demonstrate that Réotier water can enhance the skin permeability barrier in just a few hours and limit pollutants penetration and their toxicity on skin.

Conflict of Interest Statement
NONE

References.

1.   Sompornrattanaphan M. et al (2020) The contribution of particulate matter to

respiratory allergy. Asian Pac J Allergy Immunol. Mar;38(1):19-28

2.   Brook RD et al (2010) Particulate matter air pollution and cardiovascular disease: an update to the scientific statement from the American Heart Association. Circulation.121:2331–78.

3.   Li P et al (2013) The acute effects of fine particles on respiratory mortality and morbidity in Beijing, 2004–2009. Int Environ Sci Pollut Res. 20:6433–44.

4.   Drakaki E et al (2014) Air pollution and the skin. Front. Environ. Sci., vol. 2. 15 May

5.   Vierkötter A et al (2010) Airborne particle exposure and extrinsic skin aging. J Invest Dermatol ;130:2719–26.

6 .   Lee CW et al (2016) Urban particulate matter down-regulates filaggrin via COX2 expression/PGE2 production leading to skin barrier dysfunction. Sci Rep . Jun 17;6:27995

7.   Jin SP et al (2018) Urban particulate matter in air pollution penetrates into the barrier-disrupted skin and produces ROS-dependent cutaneous inflammatory response in vivo. J Dermatol Sci. Apr 30; S0923-1811(18)30202-0

8.   Morita A et al (2009) Molecular basis of tobacco smoke induced premature skin aging, J. Investig. Dermatol. Symp. Proc. 14 (1) 53–55.

9.   Ono Y et al (2013) Role of the aryl hydrocarbon receptor in tobacco smoke extract-induced matrix metalloproteinase-1 expression, Exp. Dermatol. 22 (5) 349–353.

10.   Nakamura M et al (2013) Tobacco smoke-induced skin pigmentation is mediated by the aryl hydrocarbon receptor, Exp. Dermatol. 22 (8) 556–558.

11.   Lee SH et al (1992) Calcium and potassium are important regulators of barrier homeostasis in murine epidermis. J Clin Invest. Feb;89(2):530-8.

12.   Lee SH et al (1998) Iontophoresis itself on hairless mouse skin induces the loss of the epidermal calcium gradient without skin barrier impairment. J Invest Dermatol. Jul;111(1):39-43.

13.   Hennings H et al (1980) Calcium regulation of growth and differentiation of mouse epidermal cells in culture. Cell; 19: 245-54.

14.   Tu CL and Bikle DD (2013) Role of the calcium-sensing receptor in calcium regulation of epidermal differentiation and function. Best Pract Res Clin Endocrinol Metab. Jun;27(3):415-27.

15. Wheelock MJ and Johnson KR (2003) Cadherins as modulators of cellular phenotype. Annu Rev Cell Dev Biol;19:207-35.

16. Jouret F et al (2013) Activation of the Ca2+-sensing receptor induces deposition of tight junction components to the epithelial cell plasma membrane. J Cell Sci. Nov 15;126 (Pt 22) :5132-42.

17. Cenizo V et al (2018) IFSCC congress. Full paper 344

18. Zhang Y et al (2018) Chemical composition and sources of PM 1 and PM 2.5 in Beijing in autumn. Sci Total Environ. Jul 15; 630:72-82

19. Ramirez O et al (2018) Chemical composition and source apportionment of PM 10 at an urban background site in a high-altitude Latin American megacity (Bogota, Colombia). Environ Pollut. Feb; 233:142-155.

20. Fitoussi R et al (2022) Human skin responses to environmental pollutants: A review of current scientific models. Environ Pollut. Aug 1; 306:119316

21. Pambianchi E et al (2020) Blueberry Extracts as a Novel Approach to Prevent Ozone-Induced Cutaneous Inflammasome Activation. Oxid Med Cell Longev. 9571490

22. Muharrem I and Kaplan I (2019) An Overview the Toxicology of Benzo(a)pyrene as Biomarker for Human Health: A Mini-Review. Novel Techniques in Nutrition and Food Science 2640-9208; Volume 4; Issue2

23. Crawford M and Dagnino L (2017) Scaffolding proteins in the development and maintenance of the epidermal permeability barrier. Tissue Barriers. 5(4): e1341969.

24. Chan TK et al (2021) Polycyclic aromatic hydrocarbons regulate the pigmentation pathway and induce DNA damage responses in keratinocytes, a process driven by systemic immunity. J Dermatol Sci. Nov;104(2):83-94